UDK/*UDC*: 519.6:556.166:626/627
Izvirni znanstveni članek – *Original scientific paper*

Prejeto/*Received*: 8. 1. 2015
Sprejeto/*Accepted:* 18. 4. 2015

A COMPARISON OF METHOD OF CHARACTERISTICS AND PREISSMANN SCHEME FOR FLOOD PROPAGATION MODELING WITH 1D SAINT-VENANT EQUATIONS

PRIMERJAVA METODE KARAKTERISTIK IN PREISSMANNOVE SHEME POPLAVNIH VALOV Z 1D SAINT-VENANTOVIMI ENAČBAMI

Nino Krvavica[1], Vanja Travaš[1,*]

[1] Faculty of Civil Engineering, University of Rijeka, Radmile Matejčić 3, Rijeka, Croatia

Abstract

The Saint-Venant equations were integrated by the explicit Method of Characteristics (MOC) and by the implicit Preissmann scheme to comparatively analyze and quantify the differences in prediction of flood wave propagation in open channels. For this purpose a hypothetical scenario was considered by defining a flood wave with a stage hydrograph at the inflow boundary of a prismatic channel. Downstream boundary was defined by a zero-gradient condition. The results are presented as stage hydrographs at equidistant sections along the channel. Comparative analysis revealed some differences between the compared methods. Discrepancies in peak wave heights are more evident in the upstream sections, while the downstream sections are more sensitive to differences in arrival times of flood wave peaks. The explicit MOC predicts lower wave heights and longer arrival times than the implicit Preissmann scheme.

Keywords: Saint Venant equations, method of characteristics, Preissmann scheme, flood wave propagation.

Izvleček

Saint-Venantove enačbe smo povezali z eksplicitno Metodo karakteristik in implicitno Preissmannovo shemo za potrebe primerjalne analize in ocene razlik v napovedovanju širjenja poplavnih valov v odprtih kanalih. V ta namen smo opazovali hipotetičen scenarij, pri čemer smo poplavni val opredelili s faznim hidrogramom na dotočnem robu prizmatičnega kanala. Dolvodni rob je bil določen s pogojem ničnega gradienta. Rezultate študije predstavljajo fazni hidrogrami na ekvidistantnih odsekih vzdolž kanala. Primerjalna analiza odkriva nekatere razlike med obema metodama. Razlike v konicah poplavnih valov so bolj očitne v višje ležečih odsekih, medtem ko so spodnji odseki bolj izpostavljeni razlikam v času pojava konic poplavnih valov. Eksplicitna Metoda karakteristik napoveduje nižje konice poplavnih valov in kasnejše nastope konic kot implicitna Preissmannova shema.

Ključne besede: Saint Venantove enačbe, metoda karakteristik, Preissmannova shema, širenje poplavnih valov.

[*] Stik / *Correspondence*: vanja.travas@uniri.hr

1. Introduction

The importance of developing and studying numerical procedures for predicting geometrical, kinematical and dynamical properties of flood waves is obvious and arises from the need to predict their eventual destructive and invasive interaction with the environment. Accurate prediction becomes even more evident if a flood wave travels near or through an unprotected urban area. Numerical simulations can be used to anticipate the influence of flood wave propagation on water depths in open channels, which is crucial for planning and executing essential preventive actions.

Several results of such analyses are given in terms of stage hydrographs i.e. function $h(x,t)$ that defines the water depth h at position x at time t, and flow hydrographs i.e. function $Q(x,t)$ that defines the spatial and temporal variations of the flow rate Q. However, note that the depended variables are usually assumed to be $h(x,t)$ and $v(x,t)$, since the function $Q(x,t)$ can be expressed in terms of average flow velocity $v(x,t)$ and depth $h(x,t)$. The functions $h(x,t)$ and $v(x,t)$ must satisfy the given boundary conditions and the Saint-Venant system of differential equations, derived for the considered process under a series of usually valid assumptions (Chaudhry, 2008). The system follows from the principles of conservation of linear momentum and mass. If there are no lateral inflows along the channel and a prismatic channel with rectangular cross section area is considered, the principle of mass conservation can be expressed in differential form as (Chaudhry, 2008):

$$\frac{\partial h}{\partial t} + v\frac{\partial h}{\partial x} + h\frac{\partial v}{\partial x} = 0 \qquad (1)$$

On the other hand, the linear momentum equation is usually defined by considering the gravity force component in the direction of the flow, the pressure gradient and friction force. Although some other force contributions can also be included, this gives:

$$\frac{\partial v}{\partial t} + v\frac{\partial v}{\partial x} + g\frac{\partial h}{\partial x} = g(S_0 - S_E) \qquad (2)$$

where g is gravity acceleration (m/s^2), S_0 denotes the channel bed slope and S_E denotes the slope of the energy gradient line. There are a variety of constitutive models that can be used to compute the energy loss S_0 per unit length of channel and unit weight of fluid (Subramanya, 1997). However, in the present study the Manning equation is used (Chanson, 2004; Mohan Das, 2008):

$$S_E = n^2 v^2 R^{-4/3} \qquad (3)$$

where n denotes the Manning roughness coefficient (s/m$^{1/3}$), R denotes the hydraulic radius (m) defined as A/O, where O is the cross section perimeter (m) and A is the cross section area (m^2). The latter is linearly depended on water depth h and the constant of proportionality is defined by the channel width B (m).

For given initial conditions $v_0(x,t=0)$ and $h_0(x,t=0)$ and boundary conditions, equations (1), (2) and (3) can be used to compute the flow properties over spatial domain defined between points $x=0$ and $x=L$, where L denotes the channel length, and over temporal domain from $t=0$ up to a time of interest. However, since for a general case, the solution cannot be obtained in a closed form, different numerical techniques were developed to obtain an approximated solution (Crossley, 1999).

In this paper, we focused on the Method of Characteristics (MOC) (Delphi, 2012) and the Preissmann scheme (Preissmann, 1961). A comparative analysis between the two methods was conducted and is presented hereafter. Since MOC is mainly viewed as an academic procedure (since it is difficult to adequately incorporate spatial variability) and the Preissmann scheme is widely used in practice and in several commercial software packages, the main motivation for the comparative analysis was the intention to quantify related differences, especially due to the absence of such analyses in the available literature (Shamaa, 2002; Akbari and Firoozi, 2010).

To obtain a numerical approximation of the system defined by equations (1) and (2), the spatial and temporal domains are discretized into a finite number of points. The spatial domain is discretized by a finite number n_x of computational cells with length Δx. The temporal domain is discretized by a finite number n_t of time steps Δt. To make a discrete reference on the spatial and temporal position of relevant geometrical and mechanical quantities, the subscript i is introduced to indicate their spatial position and the superscript n is introduced to denote their temporal position. The same nomenclature is hereafter used for both methods.

2. Explicit time integration by MOC

From the computational point of view, MOC is a very adequate numerical procedure that results in an efficient explicit algorithm which can be very easily implemented in any programming language. From the theoretical point of view, MOC can be used to transform a system of partial differential equations into a set of ordinary differential equations. However, note that this process is only valid for systems of hyperbolic partial differential equations such as the one that occurs in dam break problem. The essence of this method is to introduce a restriction which will specify a solution over predefined characteristics which can be geometrically interpreted as curves in the space-time domain (usually approximated by a series of straight lines). The restriction is introduced by multiplying equation (1) with an unknown quantity (Lagrange multiplier), and adding it to equation (2). After solving those equations for the unknown multiplier, the system defined by (1) and (2) can be rewritten in a compact form for the positive C^+ and negative C^- characteristic as:

$$\frac{Dv}{Dt} \pm \frac{g}{c}\frac{Dh}{Dt} = g(S_0 - S_E) \qquad (4)$$

where $c(x,t)$ denotes the wave celerity, $D\bullet/Dt$ is the material-time derivative and dx/dt denotes the slopes of the characteristic curve at some position in a space-time coordinate system in which the solutions of (4) are defined (Chanson, 2004). The resulting equation is based on the assumption that the celerity can be computed from the known depth by the gravity wave formula $c(x,t)=(g\cdot h(x,t))^{0.5}$. Moreover, this equality can be used to further simplify (4) by expressing $h(x,t)$ in terms of $c(x,t)$. Since in this case $h=c^2/g$, the derivative Dh/Dc is $2c/g$ and (4) can be rewritten as:

$$\frac{D(v \pm 2c)}{Dt} = g(S_0 - S_E) \qquad (5)$$

The material-time derivative $D(v\pm 2c)/Dt$ can be approximated by replacing the continuous space-time domain by a grid generated with a finite number of points (Figure 1). The procedure is justified from the physical point of view if the change of the quantity $(v\pm 2c)$ over time interval Δt can be assumed to be linear.

According to the previously introduced notations for spatial and temporal associations, the positive characteristic C^+ illustrated in Figure 1 between points W and P can be computed as:

$$\frac{dx}{dt} = \frac{x_i^{n+1} - x_{i-1}^n}{\Delta t} \qquad (6)$$

and the negative characteristic C^- between points E and P can be computed from:

$$\frac{dx}{dt} = \frac{x_i^{n+1} - x_{i+1}^n}{\Delta t} \qquad (7)$$

The unknown values v and c at point P can be computed from the known quantities at points W and E from the previous time level n. However, note that the slopes defined by equations (6) and (7) are only valid if the flow velocity v and celerity c can be assumed as constants inside the time interval Δt, i.e. if the characteristics can be geometrically interpreted as straight lines (Figure 1). On the other hand, for unsteady flow conditions the quantity $v\pm c$ from (5) will change in time (and space) and the start point of the characteristic curves that crosses point P will not coincide with the point W and E from the previous time step. Therefore, to compute v and c at point P, two simplifications should be introduced. The first is to

assume that the adopted time step Δt is small enough so that the characteristics for unsteady flow can still be geometrically interpreted as straight lines. If this assumption is justified (which it usually is), the second simplification is introduced so that the slope of the characteristics can be computed. Namely, if the positive characteristic from Figure 1 is considered as an example, note that the slope at point L is unknown since the velocity v_L and the celerity c_L at the same position are unknown. On the other hand, the slope of the same characteristic when it passes through point P is also unknown. The problem is usually resolved by computing the slopes using the velocity v_O and celerity c_O, i.e. the relevant quantities at the same spatial location i as point P but from the previous time step. Accordantly, the positive characteristic is defined by $\Delta x_L/\Delta t=v_O+c_O$ and the negative characteristic as $\Delta x_R/\Delta t=v_O-c_O$. For the considered case illustrated in Figure 1, the positive characteristic C^+ from equation (5) can now be rewritten in discrete form as (Chanson, 2004):

$$\frac{(v_P + 2c_P) - (v_L + 2c_L)}{\Delta t} = g(S_0 - S_E)_L \qquad (8)$$

and the negative characteristic C^- can be defined as:

$$\frac{(v_P - 2c_P) - (v_R - 2c_R)}{\Delta t} = g(S_0 - S_E)_R \qquad (9)$$

Note that the source term should also be interpolated. However, in order to retain simplicity, it can also be computed (i.e. approximated) from the known values at point L for the positive characteristic C^+ (8) and at point R for the negative characteristic C^- (9). Solving equations (8) and (9) simultaneously gives the unknown velocity v_P and celerity c_P at point P. This procedure produces an explicit algorithm that requires an additional approximation of the velocity and celerity at point L and R. However, since the relevant quantities at points W and O are known and the distance Δx_L is also known, a simple linear interpolation can be used for this purpose. The same procedure is adapted for negative characteristic C^-.

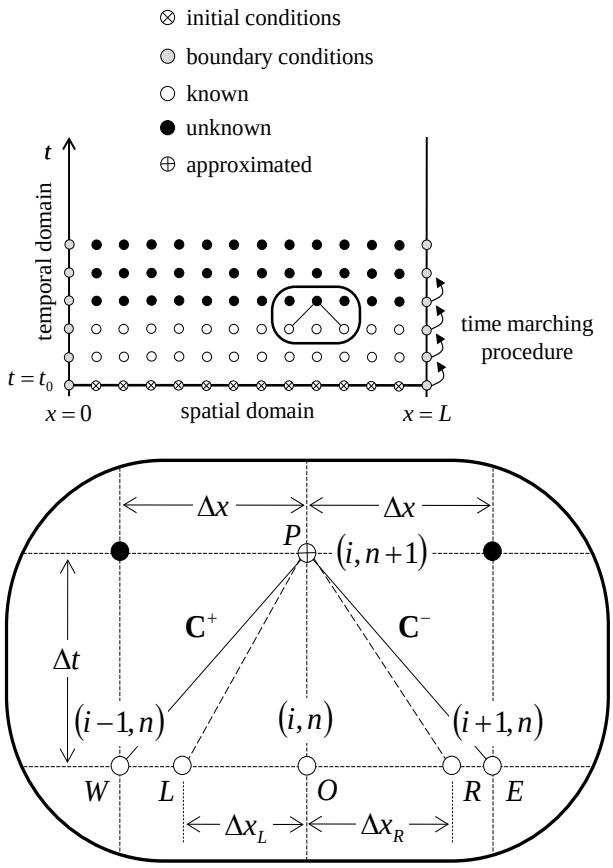

***Figure 1**: Staggered space-time grid used in MOC*

***Slika 1**: Premaknjena prostorsko-časovna mreža v metodi karakteristik*

2.1 Numerical stability

Since the numerical algorithm is explicit in time, it is only conditionally stable. The essential requirement to obtain numerical stability is prescribed by the Courant condition. In the case for flood wave propagation, it can be formulated as (Huang and Song, 1985):

$$\Delta t \leq \frac{\Delta x}{v_0 + c_0}\delta \qquad (10)$$

where δ denotes the stabilization parameter defined between 0 and 1. Besides equation (10), to secure the numerical stability, it is also necessary to meet the almost forgotten Koren condition imposed by the inequality (Huang and Song, 1985):

$$\Delta t \leq \left(\sqrt{1+2\left|\frac{v_0}{c_0}\right|}-1\right) \Bigg/ \left|\frac{v_0}{c_0}\right| \frac{gS_0}{v_0} \qquad (11)$$

For a coordinate plane with axes Δx and Δt, the inequalities (10) and (11) define a spatial region in which the pairs (Δx,Δt) will ensure a stable numerical analysis.

2.2 Boundary conditions

A stage hydrograph $h(x=0,t)$ is specified at the upstream boundary condition at $x=0$ as a Dirichlet boundary condition. Numerical treatment of the flow rate $Q(x=0,t)$ at the same cross section depends on the local Froude number Fr. Namely, for subcritical flow $Fr<1$ the flow rate $Q(x=0,t)$ can be computed from the negative characteristic (9), for supercritical flow $Fr>1$ the flow rate $Q(x=0,t)$ should also be specified in advance. At the downstream section the Neumann type of boundary condition is usually specified, in this case a zero gradient condition for both the water depth h and flow velocity v.

3. Implicit time integration by Preissmann scheme

It is commonly accepted that amongst the more popular implicit finite difference schemes (e.g. Abbot-Ionescu scheme, Vasiliev scheme, Preissmann scheme etc.) the four point implicit scheme – or box scheme – is the most robust (Cunge et al., 1980; Szymkiewicz, 2010). Because of this it is implemented in several well-known commercial software packages such as HEC-RAS (US Army Corps of Engineers, 2010) or Bentley CivilStorm (Haestad Methods Solution Center, 2011). Preissmann scheme corresponds with the box scheme when the integration point P is in the middle of the spatial increment Δx (Szymkiewicz, 2010).

With respect to the other implicit but also explicit integration methods, the main advantage of the Preissmann scheme is the ability to use variable spatial Δx_i and temporal increments Δt_n (Szymkiewicz, 2010). The spatial increment Δx_i denotes the distance between points i and i+1 and the temporal increment Δt_n denotes the time interval between the states at n and n+1. Preissmann scheme uses a non-staggered grid of points in the space-time coordinate system (Figure 2). Accordantly, a particular flow segment along the channel can be discretized more accurately (e.g. gradual change in cross section area) and the time discretization can be progressively adjusted with respect to the required temporal resolution of the results.

Before considering the numerical procedure in more detail, it is opportune to rewrite the governing differential equations in terms of a flow rate Q and water stage H which is measured from a predefined datum level. Accordantly, the continuity equation, previously defined in equation (1), can be rewritten in terms of discharge as the depended variable (conservation form) as (Szymkiewicz, 2010):

$$B\frac{\partial H}{\partial t}+\frac{\partial Q}{\partial x}=0 \qquad (12)$$

The momentum equation (2) takes the form:

$$\frac{\partial Q}{\partial t}+\frac{\partial}{\partial x}\left(\frac{\beta Q^2}{A}\right)+gA\frac{\partial H}{\partial x} = -gn^2\frac{Q|Q|}{AR^{4/3}} \qquad (13)$$

where β denotes the Boussinesq coefficient introduced to express the actual momentum in terms of average velocity v which is now contained in the depended variable Q (Szymkiewicz, 2010). The numerical procedure begins by specifying a computational grid (Figure 2).

The unknown values H and Q at time n+1 are computed with respect to the time position of point P inside the time increment Δt (Figure 2). All the derivatives, functions or algebraic expressions are computed with respect to that point. Congruently, the value of an arbitrary function $f_P(x,t)$ at point P is approximated as (Preissmann, 1961):

$$f_p(i,n) \approx \frac{1-\theta}{2}(f_{i+1}^n + f_i^n) + \frac{\theta}{2}(f_{i+1}^{n+1} + f_i^{n+1}) \quad (14)$$

where θ is the weighting parameter ranging from 0 to 1 and determines how much 'weight' is attached to the values at time level *n*+1and how much to those at time level *n*. Note that for θ=1 the computation is fully implicit in time and for θ=0 it is fully explicit. Furthermore, to obtain a numerical approximation of the system defined by equations (12) and (13), time derivatives are approximated as:

$$\frac{\partial f}{\partial t} \approx \frac{1}{2}\left(\frac{f_{i+1}^{n+1} + f_{i+1}^n}{\Delta t_n} + \frac{f_i^{n+1} + f_i^n}{\Delta t_n}\right) \quad (15)$$

and spatial derivatives as:

$$\frac{\partial f}{\partial x} \approx \theta\left(\frac{f_{i+1}^{n+1} + f_i^{n+1}}{\Delta x_i}\right) + (1-\theta)\left(\frac{f_{i+1}^n + f_i^n}{\Delta x_i}\right) \quad (16)$$

Geometrical interpretation of the weighting parameter θ is illustrated in Figure 2. With introduced approximations (15) and (16), the continuity equation (12) can be discretized in both time and space as:

$$\frac{B_p}{2}\left(\frac{H_{i+1}^{n+1} + H_{i+1}^n}{\Delta t_n} + \frac{H_i^{n+1} + H_i^n}{\Delta t_n}\right) + \theta\left(\frac{Q_{i+1}^{n+1} + Q_i^{n+1}}{\Delta x_i}\right) + (1-\theta)\left(\frac{Q_{i+1}^n + Q_i^n}{\Delta x_i}\right) = 0 \quad (17)$$

where the index *P* is introduced to denote that the width *B* is computed according to the formula given in (14). Note that for θ=0 the width B_P can be explicitly computed and interpreted as the arithmetic mean of the width of neighbouring points in the computational grid. Similarly, the momentum equation defined in (13) can be discretized to obtain:

$$\begin{aligned}&\frac{1}{2}\left(\frac{Q_{i+1}^{n+1} + Q_{i+1}^n}{\Delta t_n} + \frac{Q_i^{n+1} + Q_i^n}{\Delta t_n}\right) \\ &+\frac{\theta}{\Delta x_i}\left(\left(\frac{\beta Q^2}{A}\right)_{i+1}^{n+1} - \left(\frac{\beta Q^2}{A}\right)_i^{n+1}\right) \\ &+\frac{1-\theta}{\Delta x_i}\left(\left(\frac{\beta Q^2}{A}\right)_{i+1}^{n} - \left(\frac{\beta Q^2}{A}\right)_i^{n}\right) \\ &+gA_P\theta\left(\frac{H_{i+1}^{n+1} + H_i^{n+1}}{\Delta x_i}\right) \\ &+gA_P(1-\theta)\left(\frac{H_{i+1}^n + H_i^n}{\Delta x_i}\right) = \\ &= -\left(gn^2\frac{Q|Q|}{AR^{4/3}}\right)_P\end{aligned} \quad (18)$$

where the terms A_P, B_P and friction source term can also be computed according to the formula given in (14).

Since the cross section area *A* is a function of water stage *H*, the only unknowns are the flow rate *Q* and water stage *H* in time *n*+1. Therefore, there are only four unknowns in equations (17) and (18). To start the computation, the state at time *n* is known from the initial conditions or from the previous time step. Such a pair of equations can be written for each spatial interval Δ*x*. For a total number of n_x computational cells along the channel, the procedure defines a set of 2(n_x) algebraic equations with 2(n_x+1) unknowns, representing the values for water stage *H*(*x*,*t*) and flow rate *Q*(*x*,*t*) inside the flow domain. The resulting two equations obtained by applying the Preissmann scheme are nonlinear, due to the convective term and the friction source term, so an iterative solution technique, such as the Newton-Raphson method (Kreyszig, 2006) is required. If parameter θ is greater than zero, the computation results in a time marching procedure in which the step from one time line to the next is simultaneously performed for all points along the current time line (Figure 2).

The non-staggered space-time grid is an attractive feature of the Preissmann scheme since it can readily be used with unequal spatial increments, which is particularly important for natural waterways where channel characteristics are highly

variable even at short distances. Similarly, the applicability of unequal time steps is another important characteristic of the scheme, particularly for the case of hydrograph routing where floodwaters would generally rise relatively quickly and recess gradually in time.

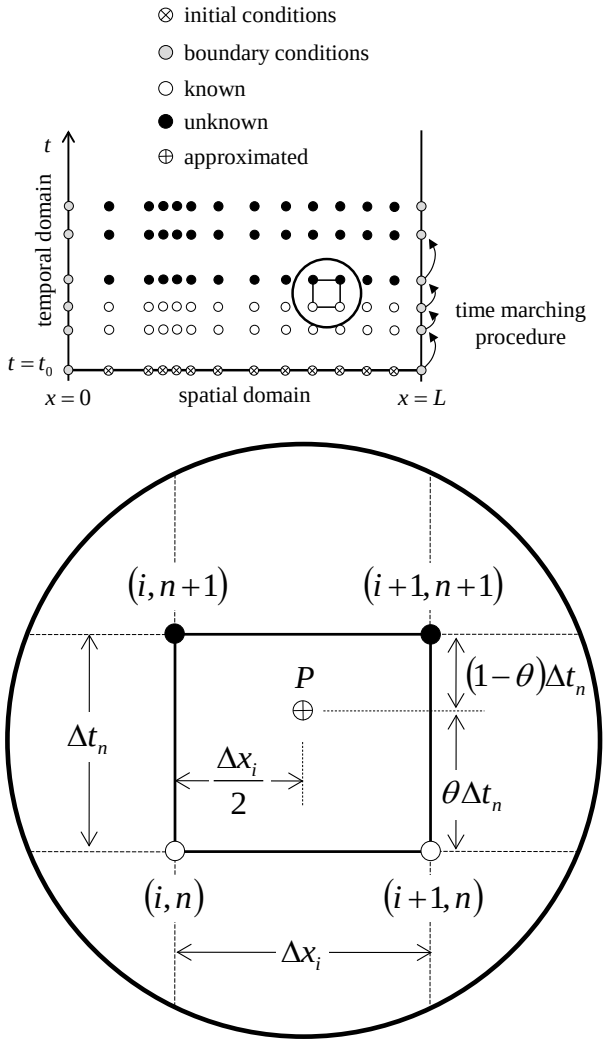

***Figure 2**: Non-staggered space-time grid used in the Preissmann scheme*

***Slika 2**: Nepremaknjena prostorsko-časovna mreža v Preissmanovi shemi*

3.1 Boundary conditions

Since this procedure defines two unknowns for each grid point with a total of $2(n_x+1)$ unknowns, and the total number of algebraic equations is $2(n_x)$, there are four additional unknowns that should be determined from the boundary conditions. So, in addition to equations (17) and (18), a unique solution of the system is obtained by defining the upstream and downstream boundary conditions. Like in the previous case, only the water stage $H(x=0,t)$ needs to be specified at the upstream cross section if $Fr<1$ and in the case of supercritical flow (i.e. if $Fr>1$), both water stage and flow rate should be specified at the same boundary. Similarly, the downstream boundary conditions are defined as zero gradient conditions for both water depth h and velocity v.

3.2 Numerical stability

The Preissmann scheme is second-order accurate in both time and space if $\theta=0.5$ and first-order accurate otherwise. Moreover, if applied to Saint-Venant system of equations, Lyn and Goodwin (1987) showed that it is unconditionally stable for $\theta>0.5$ and neutrally stable if $\theta=0.5$. For practical analysis it is common practice to set $\theta=0.55$-0.65. However, it must be mentioned that in this case the scheme gives an approximation of first-order and thus generates a numerical diffusion that can affect the numerical solution. The magnitude of diffusion depends on the values of spatial and temporal increments and the weighting parameter θ (Szymkiewicz, 2010). In other words, for $\theta>0.5$ the scheme is computationally-diffusive.

4. Comparative analysis

Major advantage of the Preissmann scheme, but also other implicit schemes, in comparison with MOC and other explicit algorithms is the fact that the numerical stability is ensured for $\theta>0.5$ (Lyn and Goodwin, 1987). In other words, the Preissmann scheme is unconditionally stable without the need to satisfy the Courant condition (10) which defines the maximum allowable time step. In spite of the fact that implicit schemes require iterations at every time step, the requirement of explicit schemes to satisfy Courant conditions often makes them less attractive in terms of computational efficiency.

However, if only computational efficiency is considered, it should also be mentioned that by increasing the number of grid points n_x the situation can be reversed. Namely, by increasing n_x the explicit time integration becomes more

attractive, since the computational efficiency of explicit algorithm reduces linearly while efficiency of implicit algorithms reduces exponentially (since it involves a solution of a system of non-linear algebraic equations).

4.1 Numerical examples

To perform a comparative analysis, the considered numerical procedures were implemented in MATLAB (2011). Those numerical algorithms were used to simulate a hypothetical scenario in which a flood wave enters from the upstream boundary in a prismatic open channel with rectangular cross section. The considered channel is L=20 km long with constant width of B=30 m.

Two different channel slopes where considered, moderately steep slope S_0=0.05 for Test Cases 1 and 2, and very mild slope S_0=0.005 for Test Cases 3 and 4. The Manning roughness coefficient was constant along the channel for all test cases and was defined as n=0.015 s/m$^{1/3}$.

The initial conditions were given as a velocity $v_0(x,t=0)$ and depth $h_0(x,t=0)$ along the flow domain ($0 \le x \le L$) at the beginning of the computational process. Since the considered channel was prismatic, i.e. characterized by constant bed slope S_0, cross section area A and roughness n, the initial conditions were defined with normal depth h_n=const. calculated for a given initial discharge Q_0. The initial flow rate Q_0 is 20 m^3/s and corresponding normal depth was computed as h_0=0.627 m for S_0=0.05 and h_0=1.27 m for S_0=0.005.

The stage hydrograph at the upstream inflow boundary was defined by a triangular shape in which the peak value h_p is reached at T_p=2 hours for Test Cases 1 and 3, or after 20 minutes for Test Cases 2 and 4. Total duration of the flood wave, or base time, was set to $T_{base}=3T_p$ for all test cases. Peak flood wave height was set to h_p=2.0 m also for all test cases (Table 1).

At the last computational node a zero gradient boundary condition is defined for both velocity v and depth h (i.e. celerity c). From the physical point of view this kind of boundary condition will describe a free boundary condition. At the numerical implementation level, this boundary condition can be simply defined by specifying that $q_{nx}=q_{nx-1}$ where q can be any relevant quantity.

The temporal domain was defined between t=0 and t=10 hours. The spatial discretization in both cases was conducted equidistantly with a total of n_x=200 number of points, which for the considered case defines the spatial increment Δx=100 m. The temporal domain was discretized by n_t=3600 time increments with individual period of Δt=10 seconds. The results of the analysis are given in Tables 2 and 3 and Figures 3a, b, c and d in which the stage hydrographs are shown for sections every 5 km along the channel.

Observing the results, differences between the methods are more obvious for milder channel slopes (Figures 3c and 3d) and for steeper flood waves (Figures 3b and 3d). The greatest differences where observed for Test Case 4 (Figure 3d).

It should be mentioned that an unexpected difference between the methods was recognized at the upstream part of the considered channel. Namely, for Test Cases 2 and 4 (steeper flood wave) the first two stage hydrographs at the upstream section are different in all the characteristics: especially the amplitude (up to 3.8%), but also in peak, rising and descending time. In the downstream part amplitudes were similar but arrival times differed significantly (up to 10.6%). Even if the time step was reduced in the explicit integration, the same differences were seen.

Table 1: *Model input parameters for all test cases*

Preglednica 1*: Vhodni modelni podatki za vse testne primere*

Test Case	Channel slope	Time to peak	Base time	Norm. depth	Peak height
nr	***S_0 (m/m)***	***T_p (s)***	***T_{base} (s)***	***h_n (m)***	***h_p (m)***
1	0,05	7200	21600	0,627	2,0
2	0,05	1200	3600	0,627	2,0
3	0,005	7200	21600	1,270	2,0
4	0,005	1200	3600	1,270	2,0

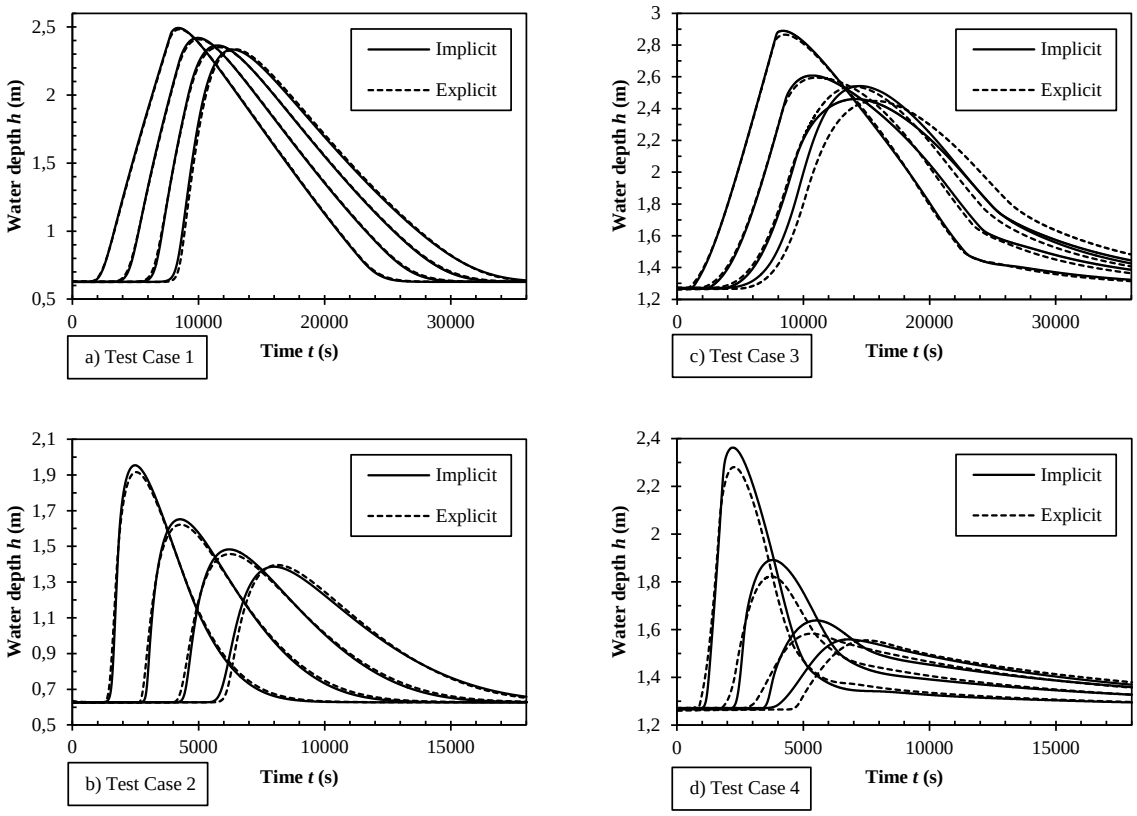

***Figure 3**: Graphical results for Test Cases a) 1, b) 2, c) 3 and d) 4, every 5 km along the channel for both MOC (Explicit) and Preissmann scheme (Implicit)*

***Slika 3**: Grafični prikaz rezultatov testnih primerov (a) 1, (b) 2, (c) 3 in (d) 4, vsakih 5 km vzdolž kanala za eksplicitno (metodo karakteristik) in implicitno (Preissmannovo) shemo*

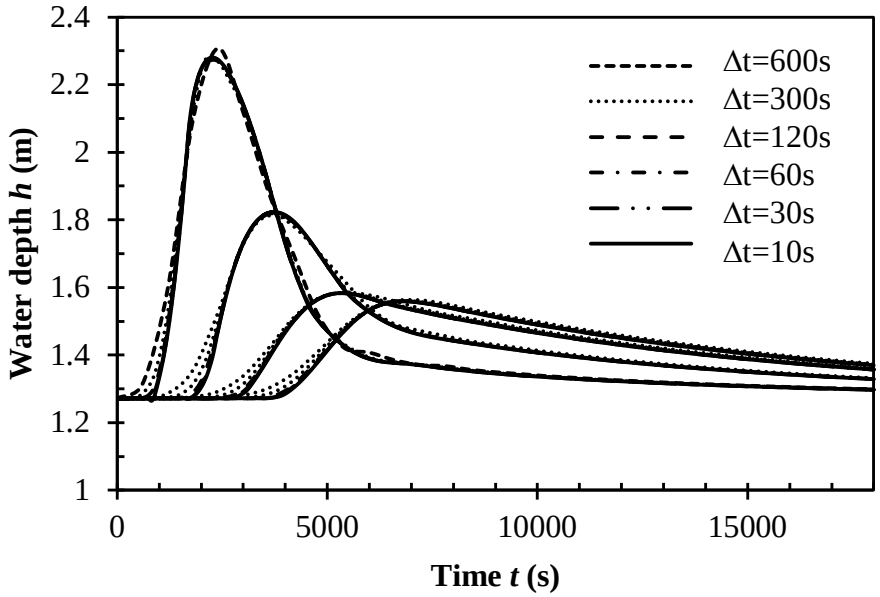

***Figure 4**: Results from Preissmann scheme for Test Case 4 with different temporal increments*

***Slika 4**: Rezultati Preissmannove sheme za primer 4 z različnimi časovnimi koraki*

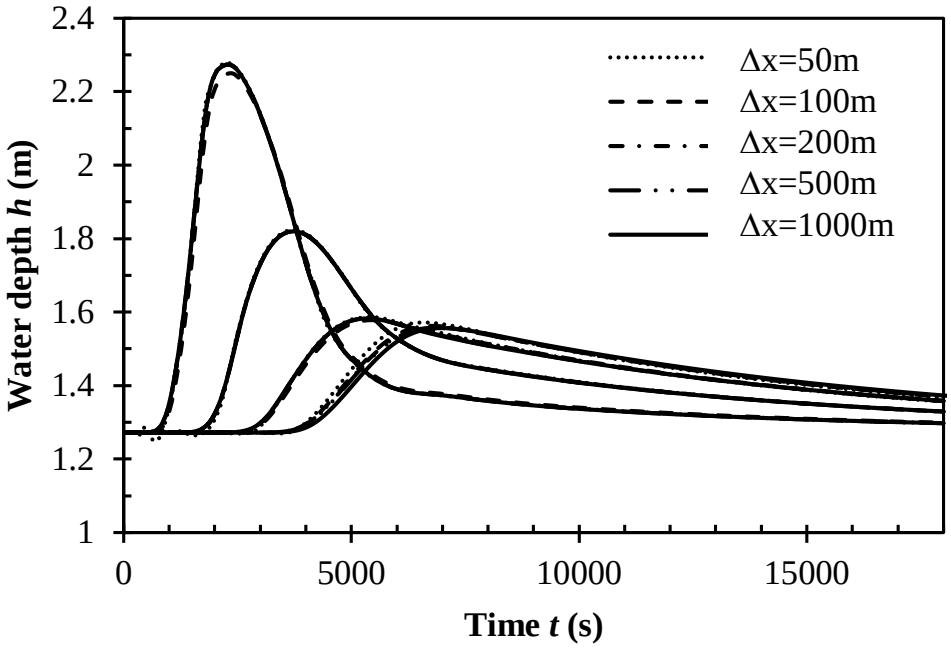

Figure 5*: Results from Preissmann scheme for Test Case 4 with different spatial increments*

Slika 5*: Rezultati Preissmannove sheme za primer 4 z različnimi prostorskimi koraki*

Table 2: *Peak wave height results for MOC and Preissmann scheme*

Preglednica 2*: Rezultati višine vala za MOC in Preissmannovo shemo*

		Preissmann	**MOC**	
Test Case	**Section**	h_p	h_p	***diff.***
nr.	**(km)**	**(m)**	**(m)**	**(%)**
1	5	2,483	2,493	0,4%
	10	2,408	2,42	0,5%
	15	2,351	2,364	0,5%
	20	2,334	2,336	0,1%
2	5	1,916	1,954	2,0%
	10	1,622	1,652	1,8%
	15	1,457	1,483	1,8%
	20	1,386	1,396	0,7%
3	5	2,865	2,89	0,9%
	10	2,595	2,608	0,5%
	15	2,539	2,46	-3,1%
	20	2,542	2,448	-3,7%
4	5	2,280	2,362	3,6%
	10	1,823	1,892	**3,8%**
	15	1,583	1,639	3,5%
	20	1,559	1,556	-0,2%

Table 3: *Arrival times of flood wave peaks for MOC and Preissmann scheme*

Preglednica 3*: Časi prihoda vala pri metodi karakteristik in Preissmannovi shemi*

		Preissmann	MOC	
Test Case	**Section**	T_p	T_p	***diff.***
nr.	**(km)**	**(s)**	**(s)**	**(%)**
1	5	8490	8410	-0,9%
	10	10030	9950	-0,8%
	15	11600	11500	-0,9%
	20	12690	12865	1,4%
2	5	2530	2485	-1,8%
	10	4300	4265	-0,8%
	15	6250	6215	-0,6%
	20	7990	8140	1,9%
3	5	8540	8385	-1,8%
	10	11090	10710	-3,4%
	15	13970	14140	1,2%
	20	14500	15695	8,2%
4	5	2270	2215	-2,4%
	10	3720	3790	1,9%
	15	5330	5525	3,7%
	20	6790	7510	**10,6%**

Generally speaking, it can be concluded that for some examples explicit time integration leads to a more diffusive results with respect to the implicit time integration which predicts stiffer flood wave propagation – higher peak amplitudes, shorter rising and peak arrival times.

4.2 Parameter selection analysis for Preissmann scheme

Influence of both temporal and spatial increments was studied for implicit Preissmann scheme to test the magnitude of expected numerical diffusivity. For Test Case 4 (which showed the largest differences between the methods) time step was altered from Δt=10 s to Δt=600 s (Figure 4), while the spatial step was altered from Δx=50 m to Δx=1000 m (Figure 5). Although some differences were observed, namely more numerically diffusive results occurred with increase in temporal and spatial increment, those differences were still much smaller in comparison to differences between explicit and implicit method.

5. Conclusion

A comparative analysis between the results obtained by MOC and Preissmann scheme for hypothetical flood wave propagation along a prismatic open channel was presented and discussed. In both cases the velocity and water depth distribution along the channel were estimated by approximating the Saint-Venant system of differential equations.

Given the same spatial and temporal increments, and considering only the computational efficiency, explicit methods are undoubtedly more suitable than the implicit ones. Moreover, the numerical implementations of the implicit methods are more complicated when a solution to a non-linear system of equations must be obtained. It should also be noted that the original Preissmann scheme is not suitable for transcritical flows (Meselhe and Holly Jr., 1997) although there are several recent adaptations that successfully solved that problem (Sart et al., 2010).

On the other hand, implicit methods are much more stable and accurate. Their greatest advantage, however, is in the freedom to choose much larger spatial and especially temporal increments, whereas explicit methods are bounded by the Courant condition.

Nevertheless, whichever method is chosen to model flood wave propagation through an open channel, selection of the appropriate numerical parameters should be considered with great care if precision and accuracy are important.

References

Akbari, G., Firoozi, B.M. (2010). Implicit and Explicit Numerical Solution of Saint-Venant Equations for Simulating Flood Wave in Natural Rivers, *5th National Congress on Civil Engineering*, Ferdowsi University of Mashhad, Mashad, Iran.

Bentley CivilStorm V8i, "User's Guide", Haestad Methods Solution Center, Watertown, USA.

Chanson, H. (2004). *The hydraulics of open channel flow: An introduction*, Second Edition, Elsevier Butterworth-Heinemann, Oxford, UK.

Chaudhry, M.H. (2008). *Open-Channel Flow*, Second Edition, Springer Science+Business Media, LLC, New York, USA.

Crossley, A. J. (1999). *Accurate and efficient numerical solution for Saint Venant equations of open channel flow*, PhD theses, University of Nottingham, UK.

Cunge, J., Holly, F.M., Verwey, A. (1980). *Practical aspects of computational river hydraulics*, Pitman Publishing, London, UK.

Delphi, M. (2012). Application of characteristics method for flood routing (Case study: Karun River), *Journal of Geology and Mining Research*, **4**(1), 8–12.

HEC-RAS 4.1 River Analysis System, (2010). "User's Manual", *US Army Corps of Engineers*, USA.

Huang, J., Song, C.C.S. (1985). Stability of Dynamic Flood Routing Schemes, *Journal of Hydraulic Engineering*, **111**(12), 1497–1505.

Kreyszig, E. (2006). *Advanced Engineering Mathematics*, 9th Edition, John Wiley & Sons Inc., USA.

Lyn, D.A., Goodwin, P. (1987). Stability of General Preissmann Scheme, *Journal of Hydraulic Engineering*, **113**(1), 16–28.

MATLAB. 2011, The MathWorks, Inc., Natick, Massachusetts, United States.

Meselhe, E.A, Holly Jr, F.M. (1997). Invalidity of Preissmann Scheme for Transcritical Flow, *Journal of Hydraulic Engineering*, **123**(7), 652–655.

Mohan Das, M. (2008). *Open channel flow*, Prentice-Hall of India Private Limited, New Delhi, India.

Preissmann, A. (1961). Propagation of translatory waves in channels and rivers, *Proc. 1st Congress of French Association for Computation*, Grenoble, France.

Sart, C., Baume, J.P., Malaterre, P.O., Guinot, V. (2010). Adaptation of Preissmann's scheme for transcritical open channel flows, *Journal of Hydraulic Research*, **48**(4), 428–440.

Shamaa, M.T. (2002). A Comparative Study of Two Numerical Methods for Regulating Unsteady Flow in Open Channels, *Mansoura Engineering Journal*, **27**(4).

Subramanya, K. (1997). *Flow in open channels*, Tata McGraw-Hill Publishing Company Limited.

Szymkiewicz, R. (2010). *Numerical Modeling in Open Channel Hydraulics*. Water Science and Technology Library, Volume 83, Springer, New York, USA.